Structure of a Mutant Form of Proliferating Cell Nuclear Antigen That Blocks Translesion DNA Synthesis[†,‡]

Bret D. Freudenthal,[§] S. Ramaswamy,[§] Manju M. Hingorani,[||] and M. Todd Washington*[,§]

Department of Biochemistry, University of Iowa College of Medicine, Iowa City, Iowa 52242-1109, and Molecular Biology and Biochemistry Department, Wesleyan University, Middletown, Connecticut 06459

Received September 17, 2008; Revised Manuscript Received October 31, 2008

ABSTRACT: Proliferating cell nuclear antigen (PCNA) is a homotrimeric protein that functions as a sliding clamp during DNA replication. Several mutant forms of PCNA that block translesion DNA synthesis have been identified in genetic studies in yeast. One such mutant protein (encoded by the *rev6-1* allele) is a glycine to serine substitution at residue 178, located at the subunit interface of PCNA. To improve our understanding of how this substitution interferes with translesion synthesis, we have determined the X-ray crystal structure of the PCNA G178S mutant protein. This substitution has little effect on the structure of the domain in which the substitution occurs. Instead, significant, local structural changes are observed in the adjacent subunit. The most notable difference between mutant and wild-type structures is in a single, extended loop (comprising amino acid residues 105−110), which we call loop J. In the mutant protein structure, loop J adopts a very different conformation in which the atoms of the protein backbone have moved by as much as 6.5 Å from their positions in the wild-type structure. To improve our understanding of the functional consequences of this structural change, we have examined the ability of this mutant protein to stimulate nucleotide incorporation by DNA polymerase eta (pol η). Steady state kinetic studies show that while wild-type PCNA stimulates incorporation by pol η opposite an abasic site, the mutant PCNA protein actually inhibits incorporation opposite this DNA lesion. These results show that the position of loop J in PCNA plays an essential role in facilitating translesion synthesis.

DNA damage in the template strand blocks replication by classical DNA polymerases, which are involved in normal DNA replication and repair. To overcome these replication blocks, cells employ several nonclassical DNA polymerases that are capable of replicating through template DNA lesions in a process called translesion DNA synthesis (*1*−*3*). One such enzyme is eukaryotic DNA polymerase eta (pol[1] η), which is a 71 kDa monomeric protein encoded by the *RAD30* gene in yeast (*4*). pol η functions in the replication of a few types of DNA lesions, including thymine dimers (*4*−*6*) and 8-oxoguanines (*7, 8*). Deletion of the *RAD30* gene in yeast leads to an increase in the level of ultraviolet (UV) radiation-induced mutagenesis (*9*−*11*), and in humans, inactivation of pol η is responsible for the variant form of xeroderma pigmentosum (XPV) (*12, 13*), which results in greater cancer susceptibility. Another nonclassical DNA polymerase in eukaryotes is DNA polymerase zeta (pol ζ), which is comprised of a 173 kDa catalytic subunit and a 29 kDa accessory subunit encoded in yeast by the *REV3* and *REV7* genes, respectively (*14, 15*). pol ζ functions in the error-prone replication of a wide range of DNA lesions, and disruptions of the *REV3* and *REV7* genes result in a drastic decrease in the frequency of DNA damage-induced mutations in yeast (*16, 17*). Moreover, expression of antisense RNA to pol ζ leads to a reduction in the frequency of UV radiation-induced mutations in human cells (*18*).

A key factor in translesion synthesis is proliferation cell nuclear antigen (PCNA). PCNA, encoded in yeast by the *POL30* gene, is a ring-shaped, homotrimeric protein that acts as a sliding clamp for classical DNA polymerases (*19, 20*). Many protein factors involved in DNA replication and repair interact with PCNA via their PCNA-interacting peptide (PIP) motifs that bind along the interdomain connector loop of PCNA (*21*). pol η binds to PCNA in this manner, and this interaction is necessary for pol η function *in vivo* (*22, 23*). Moreover, this interaction stimulates the enzymatic activity of pol η *in vitro* (*22*). pol ζ, although lacking a PIP motif, also interacts with PCNA, and its enzymatic activity is stimulated by PCNA (*24*).

Several PCNA mutant proteins in yeast have been identified that interfere with translesion synthesis in vivo (*25*−*27*). One of these is encoded by the *pol30-178* allele (formerly called the *rev6-1* allele); it encodes a mutant form of PCNA in which Gly-178 is substituted with a serine (*25*). This amino

[†] This work was supported by Grant R01GM081433 from the National Institute of General Medical Sciences.

[‡] Atomic coordinates were deposited in the RCSB Protein Data Bank as entry 3F1W.

* To whom correspondence should be addressed: Department of Biochemistry, 4-403 Bowen Science Building, University of Iowa, Iowa City, IA 52242-1109. Phone: (319) 335-7518. Fax: (319) 335-9570. E-mail: todd-washington@uiowa.edu.

[§] University of Iowa College of Medicine.

[||] Wesleyan University.

[1] Abbreviations: dNTP, deoxynucleoside triphosphate; DTT, dithiothreitol; EDTA, ethylenediaminetetraacetic acid; MMS, methyl methanesulfonate; PCNA, proliferating cell nuclear antigen; PIP, PCNA-interacting peptide; PMSF, phenylmethanesulfonyl fluoride; pol, polymerase; RFC, replication factor C; rmsd, root-mean-square deviation; UV, ultraviolet; XPV, xeroderma pigmentosum variant form.

10.1021/bi8017762 CCC: $40.75
Published on Web 11/20/2008

acid substitution is at the subunit interface of PCNA, and genetic studies have shown that translesion synthesis by both pol η and pol ζ is completely blocked in cells expressing only this mutant form of PCNA (*25*). All other aspects of DNA replication and repair appear to occur normally in cells expressing this PCNA mutant protein (*25*). Another PCNA mutant protein that blocks translesion synthesis but supports normal cell growth is encoded by the *pol30-113* allele (*26*). In this mutant protein, Glu-113 is substituted with a glycine. Interestingly, Glu-113 is also located at the subunit interface of PCNA directly opposite from Gly-178 on the neighboring subunit. On the basis of the fact that these mutant proteins block translesion synthesis without interfering with normal DNA replication, the structural changes resulting from these amino acid substitutions are likely subtle.

To understand the structural and mechanistic basis of the defect in the PCNA G178S mutant protein's ability to support translesion synthesis, we determined the X-ray crystal structure of this mutant protein to a resolution of 2.9 Å. We find that the substituted serine side chain forms a new hydrogen bond with the backbone carbonyl of Glu-113 on the adjacent subunit. This contact results in an extended loop on the adjacent subunit (comprising amino acid residues 105−110, which we call loop J), changing its conformation and moving it into an aberrant position that deviates as much as 6.5 Å from its position in the wild-type structure. We have examined the biochemical relevance of this structure by carrying out steady state kinetic studies with a model nonclassical polymerase, pol η, in the presence of the wild-type and mutant PCNA proteins. We find that while wild-type PCNA stimulates incorporation by pol η opposite an abasic site, the mutant PCNA protein inhibits incorporation opposite this DNA lesion. These findings suggest that the proper conformation of loop J is essential for translesion DNA synthesis.

EXPERIMENTAL PROCEDURES

Protein Expression and Purification. Wild-type and mutant PCNA proteins from *Saccharomyces cerevisiae* were overexpressed in *Escherichia coli* Rosetta-2 (DE3) cells harboring pET-11a vectors into which wild-type or mutant PCNA genes were cloned. PCNA proteins were N-terminally FLAG tagged for rapid purification. Transformed cells were grown at 37 °C in Overnight Express Instant TB Medium (Novagen) for 12 h. Cells were lysed in 50 mM Tris-HCl (pH 7.5), 150 mM NaCl, 1 mM PMSF, and 1 mg/mL lysozyme, with a Complete Mini Protease Inhibitor Cocktail tablet (Roche). Following ultracentrifugation, the crude extract was loaded onto a 15 mL resin bed of Anti-FLAG M2 Affinity Gel (Sigma) and purified by following the instructions. The eluted PCNA protein was then run on a Superdex G-75 column equilibrated with 20 mM Tris-HCl (pH 7.5), 1 mM DTT, and 250 mM NaCl. Yeast pol η and RFC were overexpressed and purified as previously described (*28, 29*). All purified proteins were stored in aliquots at −80 °C.

Crystallization of the PCNA G178S Mutant Protein. Crystallization of the PCNA G178S mutant protein was performed manually using the hanging drop method with 4 μL drops. To identify ideal crystallization conditions, an initial screen utilized conditions similar to those which produce wild-type PCNA crystals (*19*). Optimally diffracting crystals were generated by combining an equal volume of protein (30 mg/mL) with a reservoir solution containing 2.06 M ammonium sulfate and 0.1 M sodium citrate (pH 5.8). Cubic crystals formed within 16 h at 18 °C.

Data Collection and Structural Determination. PCNA G178S protein crystals were presoaked in a mother liquor containing 10% (v/v) glycerol prior to being flash-frozen at 100 K. Mounted crystals were subsequently used for data collection at 100 K at the 4.2.2 synchrotron beamline at the Advanced Light Source in the Ernest Orlando Lawrence Berkeley National Laboratory. The data were collected with a crystal to detector distance of 150 mm. The data were analyzed and scaled using d*trek (*30*) to a resolution of 2.9 Å, and the space group was determined to be $P2_13$, which is the same space group into which the wild-type PCNA protein crystallizes (*19*).

We carried out molecular replacement using the known structure of wild-type PCNA [Protein Data Bank (PDB) entry 1PLQ] and PHASER (*31*) to produce a model with the $P2_13$ space group. To remove any structural bias, simulated annealing was performed using PHENIX (*32*) prior to any refinement. Further structural refinement was executed using PHENIX and REFMAC5 from the CCP4 package (*31*). Model building was carried out using Coot and O (*34*). The coordinates have been deposited in the PDB as entry 3F1W.

DNA Substrates. For DNA polymerase activity assays, a synthetic 68-mer oligodeoxynucleotide with the sequence 5′-biotin-GAC GGC ATT GGA TCG ACC TCX AGT TGG TTG GAC GGG TGC GAG GCT GGC TAC CTG CGA TGA GGA CTA GC-biotin was used as the template strand (X is an abasic site or a nondamaged guanine). For the running start abasic bypass assays, a synthetic 31-mer oligodeoxynucleotide with the sequence 5′-TCG CAG GTA GCC AGC CTC GCA CCC GTC CAA C was used as a primer. For the steady state kinetic studies, a synthetic 31-mer oligodeoxynucleotide with the sequence 5′-GGT AGC CAG CCT CGC ACC CGT CCA ACC AAC T was used as a primer. Primer strands were 5′-^{32}P-end-labeled using T4 polynucleotide kinase (New England Biolabs) and [γ-^{32}P]ATP (PerkinElmer). Template strands and labeled primer strands (1 μM each) were annealed in 25 mM Tris-HCl (pH 7.5) and 100 mM NaCl by being heated to 90 °C for 2 min and slowly cooled to 22 °C over several hours. Labeled and annealed DNA substrates were stored at 4 °C for up to 2 weeks.

Polymerase Activity Assays. All experiments were conducted in 40 mM Tris-HCl (pH 7.5), 8 mM $MgCl_2$, 150 mM NaCl, 1 mM DTT, and 100 μg/mL bovine serum albumin. Reaction mixtures also contained a 10-fold molar excess of streptavidin over DNA to block the ends of the DNA to prevent PCNA dissociation. Wild-type or mutant PCNA proteins were loaded onto the DNA substrates via incubation of 90 nM PCNA (trimer concentration), 20 nM DNA, 25 nM RFC, and 500 μM ATP for 5 min at 22 °C. Reaction mixtures also contained various concentrations of dGTP (0 to 100 μM for the abasic site template) or dCTP (0 to 5 μM for the nondamaged template). Reactions were initiated via addition of 1 nM pol η and were quenched after 10 min by the addition of 10 volumes of formamide loading buffer [80% deionized formamide, 10 mM EDTA (pH 8.0), 1 mg/mL xylene cyanol, and 1 mg/mL bromophenol blue]. Extended primers (the product) and unextended primers (the substrate)

Table 1: Data Collection and Refinement Statistics

Data Collection Statistics	
resolution (Å)	29.8−2.9
wavelength (Å)	1.072
space group	$P2_13$
cell (Å)	$a = 123.13$, $b = 123.13$, $c = 123.13$
completeness (%) (last shell)	100 (3.0−2.9) (96.8)[a]
redundancy	10.79 (11.01)[a]
I/σ_I	14.8 (2.50)[a]
R_{merge} (%)[b]	7.3 (60.5)[a]
Refinement Statistics	
resolution range (Å)	19.9−2.9
R (%)[c]	22.6
R_{free} (%)[d]	25.4
rmsd for bonds (Å)	0.009
rmsd for angles (deg)	1.21
no. of water molecules	0
no. of protein atoms	1981 (254 amino acid residues)
Ramachandran analysis (%)	
most favored	89.4
allowed	10.6
PDB entry	3F1W

[a] Values in parentheses relate to the highest-resolution shell. [b] $R_{merge} = \sum I - \langle I \rangle / \sum I$, where I is the observed intensity and $\langle I \rangle$ is the average intensity obtained from multiple observations of symmetry-related reflections after rejections. [c] $R = \sum |F_o - F_c| / \sum F_o$, where F_o and F_c are the observed and calculated structure factors, respectively. [d] R_{free} is defined by Brunger (*38*).

were separated on a 15% polyacrylamide sequencing gel containing 8 M urea. The intensities of the labeled gel bands were determined using the InstantImager (Packard). The rate of product formation was graphed as a function of dNTP concentration, and the V_{max} and K_m values were obtained from the best fit of the data to the Michaelis−Menten equation using SigmaPlot 10.0.

The running start abasic site bypass assay was performed under conditions identical to those of the steady state kinetic studies except that each dNTP was used at a concentration of 20 μM. Reactions were quenched after 5, 10, and 15 min by the addition of 10 volumes of formamide loading buffer, and reaction products were visualized on a 15% polyacrylamide sequencing gel containing 8 M urea.

RESULTS

Several mutant forms of yeast PCNA that are unable to support translesion DNA synthesis in vivo have been identified in genetic screens (*25*−*27*). One of these is the PCNA G178S mutant protein. Yeast strains expressing this mutant form of PCNA have the same phenotype as strains lacking both pol η and pol ζ (*25*). To improve our understanding of how this mutant form of PCNA blocks translesion synthesis, we have determined the X-ray crystal structure of this mutant protein and have carried out functional studies of pol η in the presence of this mutant protein.

Overview of the PCNA G178S Protein Structure. We have determined the X-ray crystal structure of the PCNA G178S mutant protein to a resolution of 2.9 Å (Table 1). Figure 1A shows an overview of the structure of the PCNA G178S mutant protein trimer. Each subunit is comprised of two domains arranged in the trimeric ring in a head-to-tail fashion with domain A (residues 1−118) of one subunit interacting with domain B (residues 135−240) of its neighbor. Within each subunit, domains A and B are linked by the interdomain

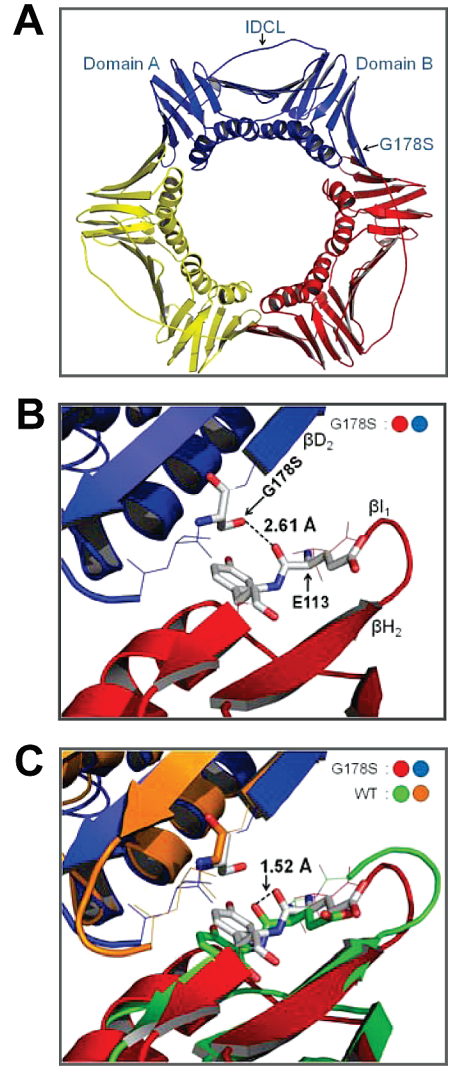

FIGURE 1: Structure of the PCNA G178S mutant protein. (A) The trimeric form of the protein is shown with monomeric subunits colored red, yellow, and blue. The interdomain connecting loop (IDCL), domains A and B, and the G178S substitution are indicated on one of the subunits. (B) Close-up, side view of the subunit interface with the Ser-178 substitution of the blue monomer and Tyr-114 and Glu-113 of the red monomer shown in stick format. The distance between the hydroxyl group of Ser-178 and the backbone carbonyl of Glu-113 is given. (C) Superimposition of the structures of the PCNA G178S mutant protein and wild-type PCNA (PDB entry 1PLQ). The distance between the backbone carbonyl group of Glu-113 in the wild-type and mutant PCNA structures is indicated.

connector loop (residues 119−134). No large-scale differences in the structure of the PCNA G178S mutant protein and the wild-type PCNA protein can be detected.

Figure 1B shows a closer view of the subunit interface of the PCNA mutant protein. The G178S substitution is located in β strand D_2 of domain B of the upper subunit. The side chain hydroxyl group of the substituted serine forms a new hydrogen bond with the backbone carbonyl of Glu-113 on the adjacent subunit. The two oxygen atoms are 2.6 Å apart, which is typical for a hydroxyl group−carbonyl group hydrogen bond. Glu-113 is in β strand I_1, which forms an antiparallel β sheet with strand H_1. In the mutant protein structure, the new hydrogen bond between Ser-178 and Glu-113 alters the trajectory of this antiparallel β sheet. This is

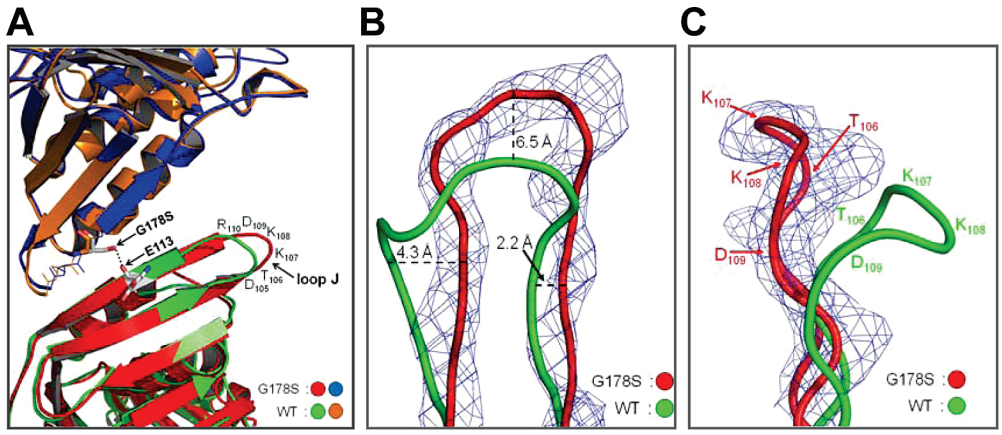

FIGURE 2: Conformation of loop J in the wild-type and mutant structures. (A) Superimposition of the wild-type and PCNA G178S mutant protein structures with the Ser-178 substitution and Glu-113 represented in stick format and the hydrogen bond between them shown as black dots. The amino acid residues of loop J are indicated. (B) Close-up view of loop J showing the electron density (level = 2.0) for the PCNA G178S mutant protein and the backbone of the wild-type and mutant proteins in ribbon representation. The distances between the wild-type and mutant protein backbone are specified. (C) Side view of loop J with the position of the amino acid residues indicated.

most clearly seen by superimposition of the structures of the wild-type and mutant PCNA proteins (Figures 1C and 2A).

Loop J in the Wild-Type and Mutant Protein Structures. Altering the trajectory of the H_1 and I_1 antiparallel β sheet results in structural changes in the extended loop between strands H_1 and I_1 (residues 105−110), which we call loop J (Figure 2A). In the mutant protein structure, this loop adopts a very different conformation in which the atoms of the protein backbone have moved significantly from their positions in the wild-type structure. For example, the α carbon of Lys-107 has moved 6.5 Å from its position in the wild-type protein structure. Figure 2B,C shows the protein backbone and electron density of loop J in its aberrant conformation in the mutant protein structure overlaid with the protein backbone of loop J in its usual conformation in the wild-type protein structure. On the basis of the clear electron density of loop J in both the wild-type and mutant protein structures, it is important to note that loop J is not merely becoming more flexible and disordered in the mutant protein structure. Instead, this loop has shifted from one stable configuration in the wild-type structure to another stable configuration in the mutant protein structure.

It should also be pointed out that the shift in loop J in this structure is not the result of crystal packing. The space group and unit cell dimensions of our crystals are the same as those reported for the wild-type protein (*19*), so observed structural differences cannot be attributed to crystal packing. Moreover, in the crystal lattice, loop J does not contact any proteins from neighboring asymmetric units; rather, it sticks out into solvent-filled spaces of the crystal lattice (see Figure S1 of the Supporting Information).

Comparison of the Two PCNA Domains. To gain insight into global structural changes occurring in PCNA as a result of the G178S substitution beyond the affected loop J, we superimposed the protein backbone of the structures of the wild-type and mutant subunits (Figure 3). Domain B which contains the G178S substitution is structurally identical to the wild-type form of PCNA. By contrast, domain A is affected by the G178S mutation on the adjacent monomer. To quantify the degree of structural difference between the wild-type and mutant forms of PCNA, we calculated rmsd values between the backbone of the wild-type and mutant

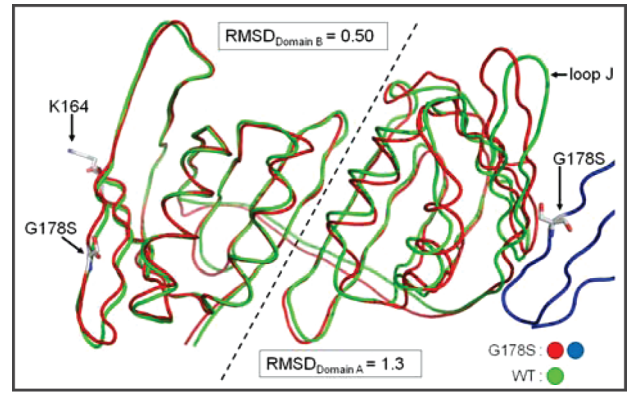

FIGURE 3: Superimposition of the PCNA monomer backbone of wild-type and mutant PCNA proteins. The monomeric subunit is lying on its side with the interdomain connector loop in the back to allow the separate domains to be easily viewed. The adjacent mutant monomeric subunit is colored blue with the G178S substitution indicated. The G178S substitution, the site of monoubiquitination (Lys-164), and loop J are indicated. Domains A and B of the monomeric subunit are separated by a dashed line, and the rmsd values were independently determined for each domain.

forms of PCNA for each domain independently. The rmsd value for the domain which contains the G178S mutation (domain B) is 0.50 Å. The rmsd value for the domain without the mutation (domain A) is 3 times as large at 1.3 Å. Thus, these results show that the G178S mutation is affecting the structure of PCNA by acting in trans to alter the structure of the neighboring monomer's domain A.

In summary, the only notable structural difference between the wild-type and mutant forms of PCNA is in domain A with the largest change being in the position of loop J. Thus, it is highly likely that the aberrant conformation of loop J is responsible for the effect of this mutation on translesion DNA synthesis.

Impact of the Mutant PCNA Protein on the Activity of pol η. Genetic studies have shown that this mutant protein blocks translesion DNA synthesis (*25*). To improve our understanding of how the structural changes described here interfere with translesion DNA synthesis, we have directly measured the enzymatic activity of the nonclassical DNA polymerase pol η in the presence and absence of wild-type

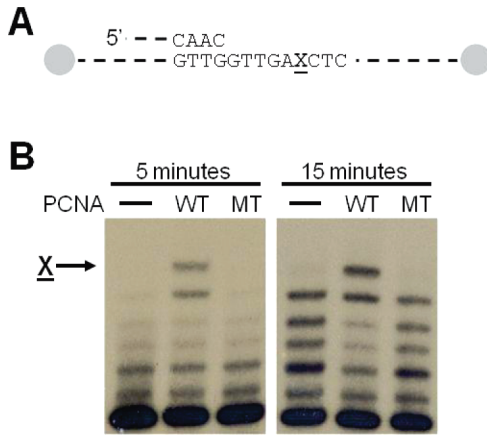

FIGURE 4: Running start experiment with pol η on an abasic site. (A) Schematic diagram of the 31/68-mer substrate used in the running start assays with the ends of the template strand containing biotin−streptavidin blocks. The X indicates the location of the abasic site. (B) Autoradiograph of the synthesis products after 5 or 15 min following the addition of pol η. The arrow indicates incorporation opposite the abasic site. Lanes labeled WT contain the wild-type PCNA protein, and lanes labeled MT contain the PCNA G178S mutant protein.

and mutant PCNA protein. Wild-type PCNA enhances the ability of pol η to incorporate nucleotides opposite an abasic site (*22*). Figure 4 shows the incorporation of pol η opposite an abasic site in a running start assay in the absence of PCNA and in the presence of either the wild-type or mutant form of PCNA. The presence of wild-type PCNA stimulates the ability of pol η to incorporate a nucleotide opposite the abasic site compared to that of pol η alone. By contrast, the mutant protein appears to have no ability to stimulate incorporation opposite the abasic site.

To quantify the effects of wild-type and mutant PCNA proteins on the enzymatic activity of pol η, we measured the kinetics of incorporation of dGTP (the preferred incoming dNTP) opposite the abasic site under steady state conditions. The rate of incorporation was plotted as a function of dGTP concentration (Figure 5); the V_{max} and K_m steady state kinetic parameters were obtained from the best fit of the data to the Michaelis−Menten equation, and these parameters are provided in Table 2. The catalytic efficiency (V_{max}/K_m) of incorporation opposite the abasic site by pol η was reproducibly 2−4-fold greater in the presence of wild-type PCNA than in the absence of PCNA, and this was due mainly to a decrease in the K_m for nucleotide incorporation. By contrast, the catalytic efficiency was not greater in the presence of the PCNA G178S mutant protein than in its absence. In fact, the catalytic efficiency was reproducibly 2−4-fold lower in the presence of the mutant PCNA than in its absence. It should be noted that like wild-type PCNA, the mutant PCNA protein also decreased the K_m for nucleotide incorporation in this context. The V_{max} for incorporation in the presence of the mutant form of PCNA, however, was ~10-fold lower than that for incorporation in its absence. Thus, the mutant form of PCNA actually inhibits the ability of pol η to incorporate nucleotides opposite abasic sites.

The inhibitory effect observed with the mutant PCNA protein requires the mutant protein to be loaded onto the primer−template DNA. We showed this by omitting either replication factor C (RFC, the ATP-dependent PCNA-loading protein) or ATP from the reaction so that the mutant PCNA protein would not be loaded onto the DNA. In these experiments, the efficiencies of nucleotide incorporation by pol η were exactly the same as those measured when no PCNA was present. For example, when we omitted ATP, the catalytic efficiency of incorporation opposite the abasic site in the presence of the unloaded mutant PCNA protein was 0.028, which is identical to the catalytic efficiency of 0.029 determined in the absence of PCNA (Table 2). Thus, we observed no inhibition of pol η-catalyzed nucleotide incorporation opposite abasic sites when the mutant form of PCNA was not loaded on the DNA substrate.

To determine whether the inhibition by this mutant PCNA protein is specific to abasic sites, we used steady state kinetics to examine if the mutant form of PCNA could inhibit the incorporation of nucleotides opposite nondamaged DNA. Figure 6 shows the rate of dCTP incorporation opposite a nondamaged G by pol η as a function of nucleotide concentration. Here again, the catalytic efficiency of incorporation opposite the nondamaged template was reproducibly 2−4-fold greater in the presence of wild-type PCNA than that in its absence (Table 2). In this case, the increased catalytic efficiency in the presence of wild-type PCNA was due to both an increase in the V_{max} and a decrease in the K_m for nucleotide incorporation in the presence of wild-type PCNA. The mutant PCNA protein inhibited the ability of pol η to incorporate opposite the nondamaged DNA to a 2−4-fold lower level of activity than pol η alone, and this was mainly due to an increase in the K_m for nucleotide incorporation. Thus, this mutant protein inhibits nucleotide incorporation by pol η opposite both damaged and nondamaged templates.

DISCUSSION

Interactions between PCNA and nonclassical polymerases have been shown to be essential for translesion synthesis. pol η possesses a PCNA-interacting peptide (PIP) motif at its extreme C-terminus (residues 621−628). While a pol η mutant protein truncated at position 624 exhibits activity in vitro, yeast expressing this truncated version of pol η have the same defect in translesion synthesis as yeast completely lacking pol η (*22*). Thus, the interaction between PCNA and pol η is essential to pol η's function in vivo. This may be because the interaction between PCNA and pol η leads to an increase in the catalytic efficiency (V_{max}/K_m) of nucleotide incorporation by pol η opposite damaged and nondamaged templates in vitro (*22*). Similarly, PCNA increases the DNA synthesis activity of pol ζ, which lacks a PIP motif, on both nondamaged DNA and UV-treated DNA (*24*). Incidentally, this also shows that there are functionally important interactions between nonclassical polymerases and PCNA that are not mediated by PIP motifs.

Translesion synthesis by both pol η and pol ζ is severely defective in yeast expressing the G178S mutant form of PCNA. This was clearly demonstrated by experiments in which plasmids containing specific DNA lesions were transformed into various yeast strains such that the transformation efficiency indicated the efficiency of DNA damage bypass (*25*). The *rev6-1* strain (expressing the G178S mutant form of PCNA) bypasses both abasic sites and *cis-syn* thymine dimers with an ~1% efficiency compared to that of the wild type (*25*). The *rev3*Δ strain (lacking pol ζ)

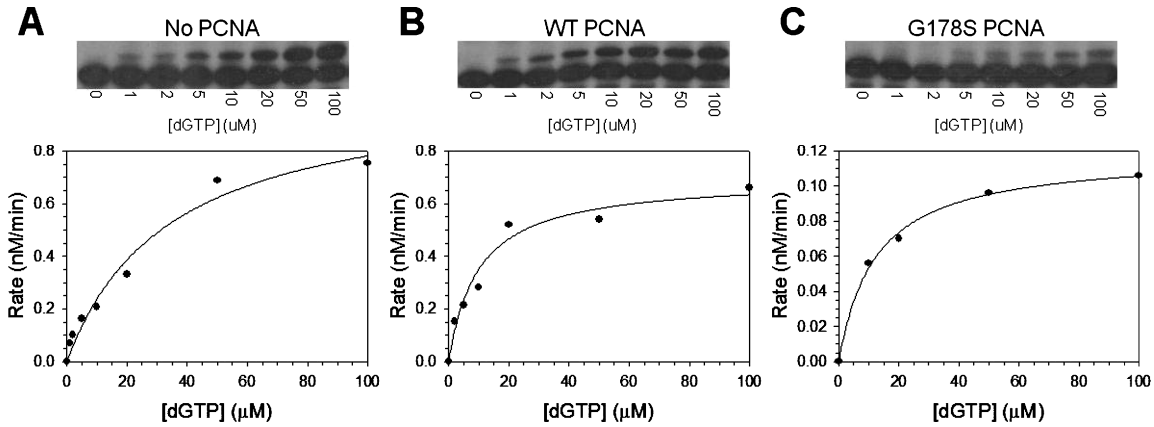

FIGURE 5: Steady state kinetics of pol η on an abasic site. The rate of nucleotide incorporation was graphed as a function of dGTP concentration for (A) pol η alone, (B) pol η with wild-type PCNA protein, and (C) pol η with the PCNA G178S mutant protein. Autoradiographs of the gels showing the incorporation of a single dGTP across from an abasic site at the indicated concentrations of nucleotide are shown above each graph. The solid lines represent the best fits of the data to the Michaelis—Menten equation, and the V_{max} and K_m steady state parameters are given in Table 2.

Table 2: Steady State Kinetic Parameters of pol η-Catalyzed Nucleotide Incorporation

protein	DNA	V_{max} (nM/min)	K_m (μM)	V_{max}/K_m	relative efficiency
pol η alone	abasic site	1.0 ± 0.1	34 ± 8	0.029	1.0
pol η with wild-type PCNA	abasic site	0.70 ± 0.06	9.9 ± 3.0	0.071	2.4
pol η with mutant PCNA	abasic site	0.12 ± 0.01	12 ± 1	0.010	0.34
pol η alone	nondamaged	3.2 ± 0.2	0.67 ± 0.12	4.8	1.0
pol η with wild-type PCNA	nondamaged	4.8 ± 0.3	0.32 ± 0.07	15	3.1
pol η with mutant PCNA	nondamaged	3.4 ± 0.3	2.1 ± 0.4	1.6	0.33

bypasses thymine dimers with an ~94% efficiency compared to that of the wild type; abasic sites are bypassed with an ~5% efficiency (*25*). The *rad30*Δ strain (lacking pol η) bypasses abasic sites with an ~80% efficiency compared to that of the wild type; *cis-syn* thymine dimers are bypassed with an ~15% efficiency (*25*). Only in the *rad30*Δ *rev3*Δ strain are the efficiencies of bypassing either of these lesions as low as they are in the *rev6-1* strain (*25*).

To improve our understanding of why the G178S substitution in PCNA leads to a loss of function of both pol η and pol ζ, but no other discernible effects on DNA replication and cell growth, we determined the X-ray crystal structure of the mutant form of PCNA to a resolution of 2.9 Å. We found that while the global structures of the wild-type and mutant protein are the same, there is a significant difference in the structure of a small region of PCNA near the subunit interface. The substituted Ser-178 side chain forms a new hydrogen bond with the backbone carbonyl of Glu-113 on the neighboring subunit. This new hydrogen bonds alters the trajectory of the β sheet comprised of strands H_1 and I_1 (containing Glu-113). This has the effect of moving loop J as much as 6.5 Å in the structure of the mutant protein from its location in the structure of the wild-type protein (Figure 2).

Since the alteration in loop J is the only significant difference between the wild-type and mutant protein structures, we conclude that the proper positioning of loop J is critical for supporting translesion synthesis by both pol η and pol ζ. Further support for this notion comes from our structural studies of the E113G mutant form of PCNA, which

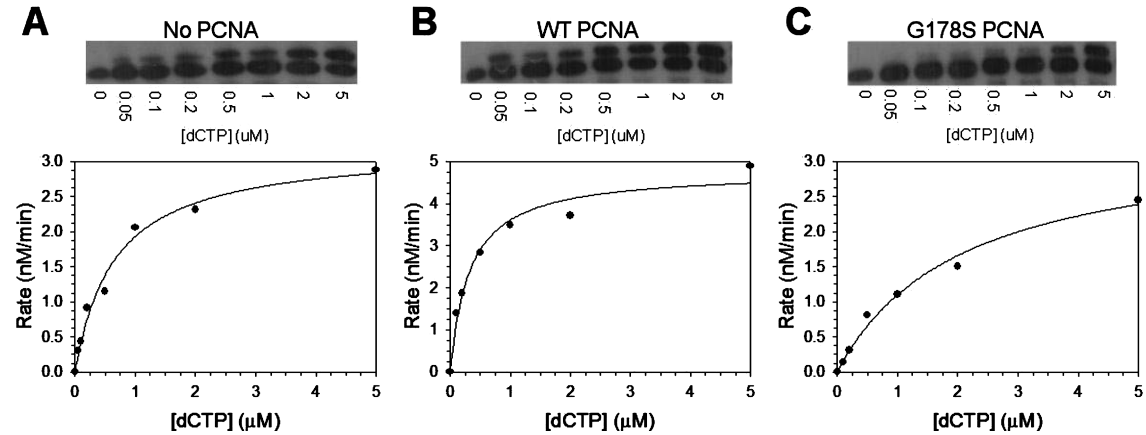

FIGURE 6: Steady state kinetics of pol η on nondamaged DNA. The rate of nucleotide incorporation was graphed as a function of dCTP concentration for (A) pol η alone, (B) pol η with wild-type PCNA protein, and (C) pol η with the PCNA G178S mutant protein. Autoradiographs of the gel showing the single incorporation of dCTP at the indicated concentrations of nucleotide are shown above each graph. The solid lines represent the best fits of the data to the Michaelis—Menten equation, and the V_{max} and K_m steady state parameters are given in Table 2.

leads to a similar defect in translesion synthesis as does the G178S mutant PCNA protein (*26*). Glu-113 is at the subunit interface directly across from Gly-178, and the side chain hydroxyl group of the G178S substitution forms a hydrogen bond with the backbone carbonyl of this residue. We have obtained crystals of the E113G mutant form of PCNA and collected X-ray diffraction data to a resolution of 3.6 Å. Comparisons of the electron densities at this resolution of the wild-type, G178S mutant, and E113G mutant proteins show that loop J is also in an aberrant configuration in the structure of the E113G mutant protein as it is in the structure of the G178S protein (see Figure S2 of the Supporting Information). Taken together, these data favor the hypothesis that loop J of PCNA makes an important direct contact with nonclassical polymerases and that when loop J adopts an aberrant conformation in the case of these two mutant proteins, this contact is disrupted.

Additional evidence of the importance of loop J comes from previous structure−function studies of PCNA. These studies have shown that several substitutions in and around loop J (residues 105−110) have been found to lead to increased sensitivity to UV radiation and the DNA-damaging agent methyl methanesulfonate (MMS) (*27*). Cells expressing the E104A/D105A double mutant have a severe defect in their ability to grow following UV or MMS treatment (*27*). Cells expressing the K108A/D109A double mutant have a minor defect in their ability to survive MMS treatment (*27*). Cells expressing the D109A/R110A double mutant have a minor defect in their ability to survive UV and MMS treatment (*27*). These studies provide additional compelling evidence that loop J of PCNA is critical for translesion DNA synthesis.

As described above, previous studies have shown that the interaction between PCNA and pol η that is mediated by the PIP motif of the polymerase is essential for translesion synthesis (*22*). It is important to note that the binding site for the PIP motif is located on the opposite face of the PCNA ring from loop J. The PIP motif binds to a hydrophobic pocket in domain B near the interdomain connector loop (*35*). Incidentally, we observe no significant structural differences between the wild-type and G178S mutant PCNA proteins in the regions of domain B or the interdomain connector loop that binds the PIP motif. Loop J is located at the subunit interface and extends out from the opposite face of the PCNA ring. These observations imply that pol η can simultaneously interact with both faces of the PCNA ring. The feasibility of this model is supported by a structure of a complex containing the "little fingers" domain of *E. coli* pol IV, which is a Y-family polymerase related to pol η, and the β-clamp processivity factor, which is structurally similar to PCNA. The C-terminal peptide of pol IV (analogous to the pol η PIP motif) binds in a pocket on one face of the β-clamp ring, and the little fingers domain of pol IV binds at the subunit interface (*36*).

To improve our understanding of how the altered conformation of loop J of PCNA affects the function of pol η, we compared the impact of the wild-type and mutant PCNA proteins on pol η's activity. We found that this mutant protein fails to stimulate the activity of pol η on both abasic sites and nondamaged templates. Not only does it fail to stimulate pol η, this mutant form of PCNA actually inhibits the activity of pol η to levels 2−4-fold lower than that of pol η in the absence of PCNA. As a result, the activity of pol η in the presence of the PCNA G178S mutant protein is approximately 10-fold lower than its activity in the presence of the wild-type PCNA protein. To the best of our knowledge, this is the first amino acid substitution in PCNA that inhibits the activity of a nonclassical DNA polymerase. It should be pointed out that the E113G mutant proteins also failed to stimulate the ability of pol η to incorporate nucleotides opposite an abasic site, although no inhibition was observed with this mutant protein (see Figure S3 of the Supporting Information). It is unclear why the G178S mutant protein inhibits pol η and the E113G protein does not. One possibility is that subtle differences in the positions of loop J between these two mutant proteins account for this difference in function. While the position of loop J is aberrant in the structures of both mutant proteins, the position of the loop is closer to that of the wild-type protein in the E113G protein structure (see Figure S3 of the Supporting Information).

It should be noted that if RFC or ATP is omitted from the reaction, no inhibition of pol η is observed with the PCNA G178S mutant protein. This shows that the inhibition requires that the mutant PCNA protein be loaded onto the DNA substrate. The precise mechanism by which the G178S mutant form of PCNA inhibits the catalytic activity of pol η is unclear, and this awaits a more detailed understanding of precisely how wild-type PCNA impacts the kinetic mechanism of nucleotide incorporation by pol η. However, one straightforward possibility is that without the requisite interaction between pol η and loop J of PCNA, the presence of PCNA on the DNA sterically interferes with the proper binding and positioning of pol η. This would prevent the formation of a productive polymerase−PCNA complex on the DNA, which may be responsible for the defect in translesion synthesis observed in cells expressing this mutant form of PCNA.

Finally, it had been suggested that the G178S substitution might block translesion synthesis by interfering with PCNA monoubiquitination (*25*), which is required for translesion synthesis (*37*). This is unlikely to be the case for several reasons. First, the site of monoubiquitination, Lys-164, is located in domain B of PCNA, which we have shown here to have the same structure in both the mutant and wild-type proteins. Second, it has previously been shown that the E113G mutant form of PCNA, which appears to block translesion synthesis by the same mechanism used by the G178S mutant protein, is capable of being monoubiquitinated in vitro by the Rad6−Rad18 complex (*26*). It should be pointed out, however, that any ability or inability of the G178S mutant protein to be monoubiquitinated is likely not relevant to understanding the mechanism by which this mutant protein blocks translesion synthesis. This is because the data presented here show that this mutant PCNA protein, even in the absence of monoubiquitination, inhibits the catalytic activity of pol η. This implies that the defect in translesion synthesis caused by this mutant protein is independent of its monoubiquitination state.

ACKNOWLEDGMENT

We thank Lokesh Gakher for providing technical assistance. We thank Lynne Dieckman, Christine Kondratick, and John Pryor for valuable discussions.

SUPPORTING INFORMATION AVAILABLE

Additional structural and kinetic data (Figures S1−S3). This material is available free of charge via the Internet at http://pubs.acs.org.

REFERENCES

1. Goodman, M. F. (2002) Error-prone repair DNA polymerases in prokaryotes and eukaryotes. *Annu. Rev. Biochem. 71*, 17–50.
2. Prakash, S., and Prakash, L. (2002) Translesion DNA synthesis in eukaryotes: A one- or two-polymerase affair. *Genes Dev. 16*, 1872–1883.
3. Prakash, S., Johnson, R. E., and Prakash, L. (2005) Eukaryotic translesion synthesis DNA polymerases: Specificity of structure and function. *Annu. Rev. Biochem. 74*, 317–353.
4. Johnson, R. E., Prakash, S., and Prakash, L. (1999) Efficient bypass of a thymine-thymine dimer by yeast DNA polymerase, Pol η. *Science 283*, 1001–1004.
5. Washington, M. T., Johnson, R. E., Prakash, S., and Prakash, L. (2000) Accuracy of thymine-thymine dimer bypass by *Saccharomyces cerevisiae* DNA polymerase η. *Proc. Natl. Acad. Sci. U.S.A. 97*, 3094–3099.
6. Washington, M. T., Prakash, L., and Prakash, S. (2003) Mechanism of nucleotide incorporation opposite a thymine-thymine dimer by yeast DNA polymerase η. *Proc. Natl. Acad. Sci. U.S.A. 100*, 12093–12098.
7. Haracska, L., Yu, S. L., Johnson, R. E., Prakash, L., and Prakash, S. (2000) Efficient and accurate replication in the presence of 7,8-dihydro-8-oxoguanine by DNA polymerase η. *Nat. Genet. 25*, 458–461.
8. Carlson, K. D., and Washington, M. T. (2005) Mechanism of efficient and accurate nucleotide incorporation opposite 7,8-dihydro-8-oxoguanine by *Saccharomyces cerevisiae* DNA polymerase η. *Mol. Cell. Biol. 25*, 2169–2176.
9. McDonald, J. P., Levine, A. S., and Woodgate, R. (1997) The *Saccharomyces cerevisiae RAD30* gene, a homologue of *Escherichia coli dinB and umuC*, is DNA damage inducible and functions in a novel error-free postreplication repair mechanism. *Genetics 147*, 1557–1568.
10. Roush, A. A., Suarez, M., Friedberg, E. C., Radman, M., and Siede, W. (1998) Deletion of the *Saccharomyces cerevisiae* gene *RAD30* encoding an *Escherichia coli* DinB homolog confers UV radiation sensitivity and altered mutability. *Mol. Gen. Genet. 257*, 686–692.
11. Johnson, R. E., Prakash, S., and Prakash, L. (1999) Requirement of DNA polymerase activity of yeast Rad30 protein for its biological function. *J. Biol. Chem. 274*, 15975–15977.
12. Masutani, C., Kusumoto, R., Yamada, A., Dohmae, N., Yokoi, M., Yuasa, M., Araki, M., Iwai, S., Takio, K., and Hanaoka, F. (1999) The XPV (xeroderma pigmentosum variant) gene encodes human DNA polymerase η. *Nature 399*, 700–704.
13. Johnson, R. E., Kondratick, C. M., Prakash, S., and Prakash, L. (1999) hRAD30 mutations in the variant form of xeroderma pigmentosum. *Science 285*, 263–265.
14. Morrison, A., Christensen, R. B., Alley, J., Beck, A. K., Bernstine, E. G., Lemontt, J. F., and Lawrence, C. W. (1989) *REV3*, a *Saccharomyces cerevisiae* gene whose function is required for induced mutagenesis, is predicted to encode a nonessential DNA polymerase. *J. Bacteriol. 171*, 5659–5667.
15. Nelson, J. R., Lawrence, C. W., and Hinkle, D. C. (1996) Thymine-thymine dimer bypass by yeast DNA polymerase η. *Science 272*, 1646–1649.
16. Johnson, R. E., Washington, M. T., Haracska, L., Prakash, S., and Prakash, L. (2000) Eukaryotic polymerase ι and ζ act sequentially to bypass DNA lesions. *Nature 406*, 1015–1019.
17. Lawrence, C. W. (2002) Cellular roles of DNA polymerase ζ and Rev1 protein. *DNA Repair 1*, 425–435.
18. Gibbs, P. E. M., McGregor, W. G., Maher, V. M., Nisson, P., and Lawrence, C. W. (1998) A human homolog of the *Saccharomyces cerevisiae REV3* gene, which encoded the catalytic subunit of DNA polymerase ζ. *Proc. Natl. Acad. Sci. U.S.A. 95*, 6876–6880.
19. Krishna, T. S., Kong, X. P., Gary, S., Burgers, P. M., and Kuriyan, J. (1994) Crystal structure of the eukaryotic DNA polymerase processivity factor PCNA. *Cell 79*, 1233–1243.
20. Langston, L. D., and O'Donnell, M. (2008) DNA polymerase δ is highly processive with PCNA and undergoes collision release upon completing DNA. *J. Biol. Chem. 283*, 29522–29531.
21. Hingorani, M. M., and O'Donnell, M. (2000) Sliding clamps: A (tail)ored fit. *Curr. Biol. 10*, R25−R29.
22. Haracska, L., Kondratick, C. M., Unk, I., Prakash, S., and Prakash, L. (2001) Interaction with PCNA is essential for yeast polymerase η function. *Mol. Cell 8*, 407–415.
23. Haracska, L., Johnson, R. E., Unk, I., Phillips, B., Hurwitz, J., Prakash, L., and Prakash, S. (2001) Physical and functional interactions of human DNA polymerase η with PCNA. *Mol. Cell. Biol. 21*, 7199–7206.
24. Garg, P., Stith, C. M., Majka, J., and Burgers, P. M. J. (2005) Proliferating cell nuclear antigen promotes translesion synthesis by DNA polymerase ζ. *J. Biol. Chem. 280*, 23446–23450.
25. Zhang, H., Gibbs, P. E. M., and Lawrence, C. W. (2006) The *Saccharomyces cerevisiae rev6-1* mutation, which inhbits both the lesion bypass and the recombination mode of DNA damage tolerance, is an allele of POL30, encoding proliferating cell nuclear antigen. *Genetics 173*, 1983–1989.
26. Northam, M. R., Garg, P., Baitin, D. M., Burgers, P. M. J., and Shcherbakova, P. V. (2006) A novel function of DNA polymerase ζ regulated by PCNA. *EMBO J. 25*, 4316–4325.
27. Ayyagari, R., Impellizzeri, K. J., Yoder, B. L., Gary, S. L., and Burgers, P. M. J. (1995) A mutational analysis of the yeast proliferating cell nuclear antigen indicates distinct roles in DNA replication and repair. *Mol. Cell. Biol. 15*, 4420–4429.
28. Washington, M. T., Prakash, L., and Prakash, S. (2001) Yeast DNA polymerase η utilizes an induced-fit mechanism of nucleotide incorporation. *Cell 107*, 917–927.
29. Finkelstein, J., Antony, E., Hingorani, M. M., and O'Donnell, M. (2003) Overproduction and analysis of eukaryotic multiprotein complexes in *Escherichia coli* using a dual-vector strategy. *Anal. Biochem. 319*, 78–87.
30. Pflugrath, J. W. (1999) The finer things in X-ray diffraction data collection. *Acta Crystallogr. D55*, 1718–1725.
31. Read, R. J. (2001) Pushing the boundaries of molecular replacement with maximum likelihood. *Acta Crystallogr. D57*, 1373–1382.
32. Adams, P. D., Grosse-Kunstleve, R. W., Hung, L. W., Ioerger, T. R., McCoy, A. J., Moriarty, N. W., Read, R. J., Sacchettini, J. C., Sauter, N. K., and Terwilliger, T. C. (2002) PHENIX: Building new software for automated crystallographic structure determination. *Acta Crystallogr. D58*, 1948–1954.
33. Collaborative Computational Project, Number 4 (1994) The CCP4 Suite: Programs for Protein Crystallography. *Acta Crystallogr. D50*, 760–763.
34. Emsley, P., and Cowtan, K. (2004) Coot: Model-building tools for molecular graphics. *Acta Crystallogr. D60*, 2126–2132.
35. Brunning, J. B., and Shampoo, Y. (2004) Structural and thermodynamic analysis of human PCNA with peptides derived from DNA polymerase-δ p66 subunit and flap endonuclease-1. *Structure 12*, 2209–2219.
36. Bunting, K. A., Roe, S. M., and Pearl, L. H. (2003) Structural basis for recruiting of translesion DNA polymerase Pol IV/DinB to the β-clamp. *EMBO J. 22*, 5883–5892.
37. Hoege, C., Pfander, B., Moldovan, G. L., Pyrowolaksi, G., and Jentsch, S. (2002) RAD6-dependent DNA repair is linked to modification of PCNA by ubiquitin and SUMO. *Nature 419*, 135–141.
38. Brunger, A. T. (1992) Free R value: A novel statistical quantity for assessing the accuracy of crystal structures. *Nature 355*, 472–475.

BI8017762